A general approach for sharp crystal phase switching in InAs, GaAs, InP, and GaP nanowires using only group V flow

Sebastian Lehmann[1], Jesper Wallentin[1], Daniel Jacobsson[1], Knut Deppert[1], and Kimberly A. Dick[1,2]

[1] *Solid State Physics, Lund University, Box 118, S-221 00 Lund, Sweden,*

[2] *Polymer & Materials Chemistry, Lund University, Box 124, S-221 00 Lund, Sweden*

Supplementary Information:

S1 Methods:

III-V heterostructured nanowires (NWs) were prepared by metal-organic vapor phase epitaxy (MOVPE) following the particle-assisted growth mode and the use of Au particles. The latter were deposited onto $[\bar{1}\bar{1}\bar{1}]$-oriented III-V (III=Ga,In) (V=P,As) substrates by aerosol technique[1] with an areal density of 1.0 μm^{-2} and diameters in the range of 30-80 nm. The NWs were grown at temperatures of 580°C (GaP), 550°C (GaAs), 480°C (InP), and 460°C as well as 415°C (InAs) with trimethylgallium (TMGa), trimethylindium (TMIn), phosphine (PH_3) and arsine (AsH_3) as precursor materials at total reactor flows of 13slm at a total reactor pressure of 100 mbar. The molar fractions were set to $\chi_{\mathrm{TMGa}}= 4.3\mathrm{x}10^{-5}$ and $\chi_{\mathrm{PH_3}}= 1.9\mathrm{x}10^{-4}$ - $2.5\mathrm{x}10^{-2}$ for GaP growth, to $\chi_{\mathrm{TMGa}}= 4.3\mathrm{x}10^{-5}$ and $\chi_{\mathrm{AsH_3}}= 7.7\mathrm{x}10^{-5}$ - $3.9\mathrm{x}10^{-3}$ for GaAs growth, to $\chi_{\mathrm{TMIn}}= 6.1\mathrm{x}10^{-6}$ and $\chi_{\mathrm{PH_3}}= 1.5\mathrm{x}10^{-4}$ - $1.5\mathrm{x}10^{-2}$ for InP growth, and to $\chi_{\mathrm{TMIn}}= 6.1\mathrm{x}10^{-6}$ and $\chi_{\mathrm{AsH_3}}= 2.7\mathrm{x}10^{-5}$ - $1.5\mathrm{x}10^{-3}$ for InAs growth. In order to remove surface oxides and allow proper substrate preconditioning a 10min annealing step was carried out prior to growth at 630°C (GaP, GaAs) and 550°C (InP, InAs), respectively, in AsH_3/H_2 or PH_3/H_2 atmosphere. After that step the temperature was reduced to growth temperature and after thermal stabilization the precursors were introduced to initiate growth. Nominal [V]/[III]-ratios of the incoming precursor flows of 1.8 - 31 for WZ and 90 - 2515 for ZB growth conditions were used. After growth the samples were cooled in either AsH_3/H_2 or PH_3/H_2 mixture or hydrogen only.

SEM characterization was carried out in a ZEISS Leo Gemini 1560 setup. For structural characterization the nanowires were placed on copper grids covered with a lacey carbon layer and investigated in a JEOL-3000F transmission electron microscope (TEM) with at least 4 wires imaged for each sample investigated.

S2: Growth rates of WZ and ZB in GaP, GaAs, InP, and InAs NWs:

The growth rates of WZ and ZB segments are summarized in table 1 determined from various single and multiple heterostructured NWs. The integrated ZB growth rate is always lower than the corresponding WZ growth rate, roughly by a factor of 2 except for the case of GaP. The deviating behavior of GaP could be explained by strongly increased radial growth rates due to the high temperature (580°C) and the high group V molar flow for ZB growth conditions (see S4 further below). However, independently we have extensively explored the growth of InAs axial heterostructures using the same approach of just switching group V flow for crystal structure control with the result of similar growth rates for both, the ZB and WZ segment (Unfortunately this is not within the scope of this report and will be reported in the near future). Thus, we assume that the observed difference in growth rates stems from materials competition during ZB growth which arises mainly from enhanced substrate and enhanced lateral ⟨110⟩-directional growth of the ZB top part of the nanowires (figure 4) – or consumed for WZ stem overgrowth for the case of GaP. This has been reported earlier as a consequence of nominally high [V]/[III]-ratios[2–4], however, differences in crystal structure and wire terminating facets were reported for NW growth as well[5–7].

	growth rate WZ $\left(\frac{\text{nm}}{\text{min}}\right)$	growth rate ZB $\left(\frac{\text{nm}}{\text{min}}\right)$
GaP (580°C)	138	3
GaAs (550°C)	120	61
InP (480°C)	23	12
InAs (460°C)	60	40
InAs (415°C)	17	6

Table S2: Growth rate for WZ and ZB of GaAs, InAs, GaP, and InP as determined for single and multiple heterostructured NWs.

S3: Particle compositions:

Particle compositions were determined ex-situ for WZ and ZB wires which were cooled either in hydrogen or AsH_3/H_2 or PH_3/H_2 atmosphere. We found different [Au]/[III]-ratios in the particle for WZ and ZB wires when cooled under hydrogen and similar ones when cooled in the presence of group V hydrides, but The ex-situ composition has to be interpreted with care[8]. However, during hydrogen cool-down we cannot exclude the post-growth group-III enrichment of the particle stemming from material still present at the surfaces or available due to minor catalytic decomposition of the III-V material by available liquid indium, gallium or Au_xIII_{1-x}-alloys[9–11]. This effect would probably be higher at higher growth temperatures like e.g. in the case of GaAs and GaP as well as for WZ growth with very low nominal [V]/[III]-ratios. The assumptions are actually supported by the compositional data for InAs grown at 460°C and 415°C. For these experiments both, the absolute group III concentration in the particle decreases as well as the difference between WZ and ZB NW particle compositions. Thus we assume that the Au_xIII_{1-x} particle compositions were similar for the cases of WZ and ZB growth.

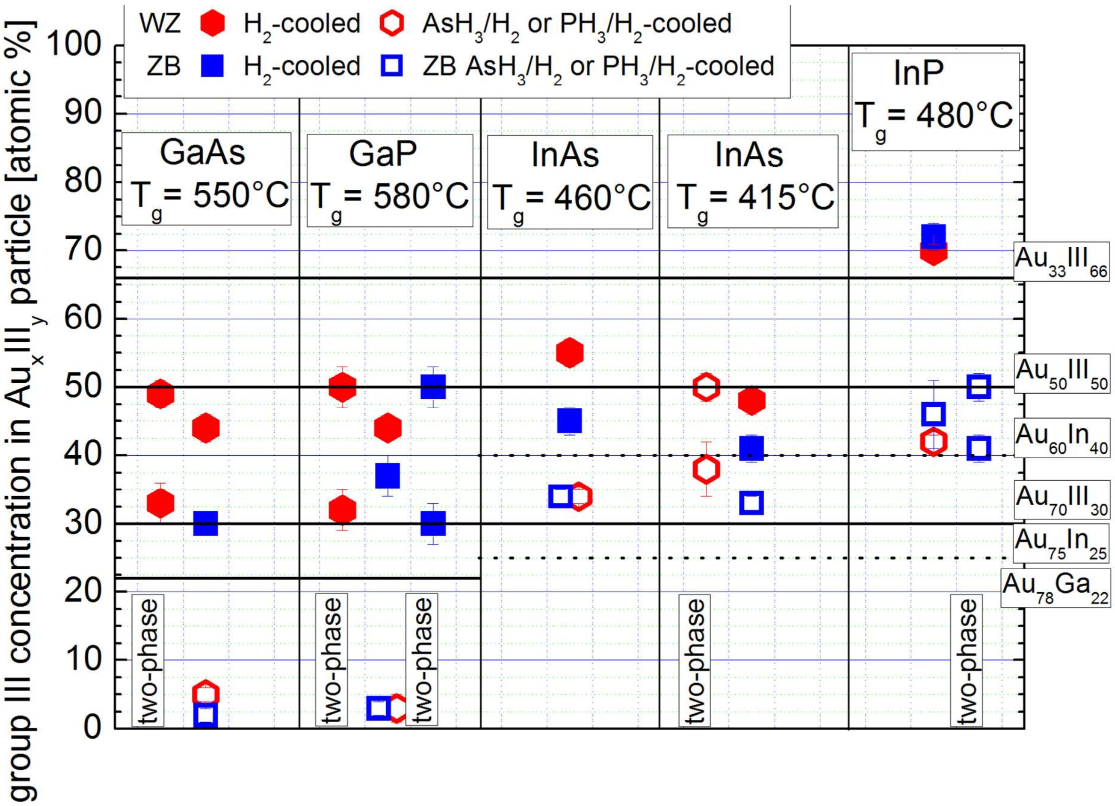

Figure S3: Particle composition of Au-III alloy particles for GaAs (550°C), GaP (580°C), InAs (415°C and 460°C), as well as for InP (480°C). The compositional analysis was carried out ex-situ by TEM EDX and all samples were cooled in AsH_3/H_2 and PH_3/H_2 atmosphere, respectively, or in H_2 only. Additionally, lines are given indicating the equilibrium Au-alloy phases according to the corresponding phase diagrams[53]. In case the particles consisted of two different phases the compositions of those are given in addition to the average compositional data.

S4: GaP morphology

Why exactly the GaP heterostructures show a significant morphological deviation from the other materials – meaning a larger diameter of the WZ bottom part compared to the ZB top part – we can only speculate. The most probable answer is the decreased migration length of involved growth species due to i.) the high growth temperature of 580°C, ii.) the generally low mobility of PH_3-related species at the substrate surface and NW side facets, and iii.) an increased number of stacking defects in the WZ bottom segment which act as nucleation centers and additionally promote radial overgrowth. Point iii.) is supported by the BF TEM image in figure 1 a. where step like features are to be seen at axial positions of the NW where stacking defects are present in the bottom WZ segment. Although rather different ZB morphologies occurred for heterostructured NWs of GaP and GaAs, still points i.) and ii.) are supported by the comparison between both. First, the growth temperature of GaAs NWs was slightly lower (550°C) and second, the migration length of AsH_3-related species might in general be higher compared to the PH_3-related counterparts as indicated by the more tapered morphology of the GaAs WZ bottom segment but still remarkable substrate growth.

References:

(1) Magnusson, M. H.; Deppert, K.; Malm, J.-O.; Bovin, J.-O.; Samuelson, L. *Nanostructured Materials* **1999**, *12*, 45–48.

(2) Dick, K. A.; Deppert, K.; Samuelson, L.; Seifert, W. *Journal of Crystal Growth* **2006**, *297*, 326–333.

(3) Seifert, W.; Borgström, M.; Deppert, K.; Dick, K. A.; Johansson, J.; Larsson, M. W.; Mårtensson, T.; Sköld, N.; Patrik T. Svensson, C.; Wacaser, B. A.; Reine Wallenberg, L.; Samuelson, L. *Journal of Crystal Growth* **2004**, *272*, 211–220.

(4) Asai, H. *Journal of Crystal Growth* **1987**, *80*, 425–433.

(5) Poole, P. J.; Dalacu, D.; Wu, X.; Lapointe, J.; Mnaymneh, K. *Nanotechnology* **2012**, *23*, 385205.

(6) Gorji Ghalamestani, S.; Heurlin, M.; Wernersson, L.-E.; Lehmann, S.; Dick, K. A. *Nanotechnology* **2012**, *23*, 285601.

(7) Wallentin, J.; Messing, M. E.; Trygg, E.; Samuelson, L.; Deppert, K.; Borgström, M. T. *Journal of Crystal Growth* **2011**, *331*, 8–14.

(8) Persson, A. I.; Larsson, M. W.; Stenstrom, S.; Ohlsson, B. J.; Samuelson, L.; Wallenberg, L. R. *Nat Mater* **2004**, *3*, 677–681.

(9) Schoonmaker, R. C.; Buhl, A.; Lemley, J. *J. Phys. Chem.* **1965**, *69*, 3455–3460.

(10) Lou, C. Y.; Somorjai, G. A. *The Journal of Chemical Physics* **1971**, *55*, 4554–4565.

(11) Thomas, T. C.; Williams, R. S. *Journal of Materials Research* **1986**, *1*, 352–360.